ENO2 affects the EMT process of renal cell carcinoma and participates in the regulation of the immune microenvironment

WEI-JIE CHEN[1,2*], WEI YANG[1,2*], MIN GONG[3*], YI HE[4*], DA XU[1], JIA-XIN CHEN[1], WEN-JIN CHEN[1], WEN-YAN LI[2], YU-QI WANG[2], KE-QIN DONG[1], XU SONG[3], XIU-WU PAN[1,2] and XIN-GANG CUI[1,2]

[1]Department of Urology, Third Affiliated Hospital of The Second Military Medical University, Shanghai 200433; [2]Department of Urology, Xinhua Hospital, Shanghai Jiaotong University School of Medicine, Shanghai 200092; [3]Department of Urology, Seventh People's Hospital of Shanghai University of Traditional Chinese Medicine, Shanghai 200137; [4]Department of Urology, Jiaxing First Hospital, Jiaxing, Zhejiang 314001, P.R. China

Received August 3, 2022; Accepted October 20, 2022

DOI: 10.3892/or.2022.8470

Abstract. Clear cell renal cell carcinoma (ccRCC) is a frequent malignant tumor of the kidney which has a dismal prognosis. At present, targeted therapies and immunotherapy have achieved significant results; however, the overall survival rate of patients with ccRCC remains unacceptably poor. It is therefore necessary to find novel therapeutic and diagnostic targets for ccRCC. It has been reported that enolase 2 (ENO2) is an oncogene, although its function in the immune microenvironment and in the growth of ccRCC has yet to be fully elucidated. The present study analyzed the data of patients with ccRCC both from the Gene Expression Omnibus (GEO) and The Cancer Genome Atlas (TCGA) databases, and from clinical samples obtained from Third Affiliated Hospital of the Second Military Medical University to investigate the role of ENO2 in the progression of ccRCC and the correlation between ENO2 and certain clinical features. It was found that the expression of ENO2 was elevated both in patients with ccRCC retrieved from the GEO and TCGA databases and in clinical ccRCC samples obtained from Third Affiliated Hospital of the Second Military Medical University. In addition, the prognosis of patients was poorer when ENO2 was highly expressed. Gene Ontology (GO) analysis and Gene Set Enrichment Analysis (GSEA) confirmed that ENO2 participated in the regulation of various pathways in ccRCC. *In vitro* experiments including Cell Counting Kit-8 cell proliferation assay, Transwell and Matrigel assays confirmed that ENO2 could promote the proliferation and migration of ccRCC cells. Furthermore, a number of immunosuppressive indicators were identified that positively correlated with ENO2 expression. In conclusion, the present study revealed that ENO2 expression promotes the proliferation, invasion and migration of ccRCC cells, and may serve as a novel predictor to evaluate prognosis and the efficacy of immune checkpoint blockade treatment for patients with ccRCC.

Correspondence to: Dr Xin-Gang Cui, Department of Urology, Third Affiliated Hospital of The Second Military Medical University, 225 Changhai Road, Shanghai 200433, P.R. China
E-mail: cuixingang@xinhuamed.com.cn

Dr Xiu-Wu Pan, Department of Urology, Xinhua Hospital, Shanghai Jiaotong University School of Medicine, 1665 Kongjiang Road, Shanghai 200092, P.R. China
E-mail: panxiuwu@126.com

*Contributed equally

Key words: clear cell renal cell carcinoma, enolase 2, prognosis, cancer progression, epithelial-mesenchymal transition, immune microenvironment, immune checkpoint therapy

Introduction

Renal cell carcinoma (RCC), which originates from renal tubular epithelium, has become one of the most commonly occurring malignant tumors. Over the course of the last 20 years, the incidence rate of RCC has been on the rise, accounting for ~2-3% of all new cancer patients (1). Renal clear RCC (ccRCC) is the main subtype of RCC (2). Regrettably, numerous patients with ccRCC are diagnosed with advanced tumors, and 25-30% of patients are identified as having tumor metastasis at the time of diagnosis (3). At present, the great strides that have been made in terms of comprehensive treatment strategies have greatly improved the prognosis of patients with ccRCC, although these treatment schemes have poor efficacy for certain patients (1,4). Consequently, there is an urgent need to find novel markers for the diagnosis and prediction of curative effect of ccRCC.

The development of bioinformatics analysis in recent years has rendered it possible to explore gene regulatory networks (5). In the present study, differentially expressed genes (DEGs) were screened from GSE40435, protein-protein interaction (PPI) analysis was subsequently used to determine the interaction between DEGs, and finally a cytoHubba plug-in was used to identify hub genes in Cytoscape. These hub genes were verified through multiple databases, which enabled the target gene enolase (ENO2) to be ultimately selected.

ENO2, also known as neuron specific enolase (NSE), is mainly distributed in neuroendocrine cells. It is recognized

as a tumor marker that fulfills an important role in tumor development (6). ENO2 is highly expressed in glioblastoma cells, wherein it activates the PI3K/Akt and anti-apoptotic signaling pathways (7,8). In glioblastoma cells, ENO2 has also been shown to indirectly regulate the participation of actin in tumor migration (9,10). In addition, the serum ENO2 level may be used as a prognostic marker for patients with pancreatic endocrine tumors and melanoma (11). Another recently published study reported that ENO2 overexpression impacts the prognosis of patients with ccRCC through participating in the glycolytic process of cancer cells in papillary RCC (12). The aim of the present study was to examine the potential role and function of ENO2 in the immune microenvironment and in the growth of ccRCC. During the course of this study, it was identified that ENO2 is highly expressed in ccRCC, acting as an independent risk factor for predicting the prognosis of patients. A series of *in vitro* experiments showed that knockdown of ENO2 could affect the epithelial-mesenchymal transition (EMT) process of tumors, and inhibit the migration and proliferation of ccRCC cell lines. Finally, it was found that the expression of ENO2 is closely associated with tumor immune infiltration, and may affect the effects of immune checkpoint blockade (ICB) in patients with ccRCC.

Materials and methods

Public data acquisition. The Gene Expression Omnibus (GEO) database (https://www.ncbi.nlm.nih.gov/geo/) was used to query the gene expression information of the GSE40435, GSE46699 and GSE53757 datasets. The clinicopathological data and RNA-sequencing (RNA-seq) data of 531 patients with ccRCC were obtained from The Cancer Genome Atlas (TCGA) database (https://portal.gdc.cancer.gov/).

PPI analysis. The STRING website (https://string-db.org/cgi/) was utilized for PPI analysis (13), and the 30 top hub genes were identified through Cytoscape (14,15).

Patients and specimens. The present study was approved (approval no. EHBHKY2021-01-005) by the ethics committee of Second Military Medical University (Shanghai, China). Written informed consent was obtained from all patients. Clinical specimens of RCC, together with paired adjacent tissues, were collected from 191 patients who underwent surgical treatment in the urology department of Third Affiliated Hospital of the Second Military Medical University (Shanghai, China) between October 2014 and February 2019. Clinicopathological variables of these samples were collected, as shown in Table SI. Two pathologists evaluated the pathological characteristics of ccRCC.

Immunohistochemistry (IHC) analysis. IHC was performed according to the previously described protocol (16) using rabbit anti-ENO2 antibody (1:1,000; cat. no. ab79757; Abcam). The score of staining intensity was defined as follows: Negative, 0; weak, 1; moderate, 2; and strong, 3. The frequency of positive cells was defined as follows: <5, 0; 5-25, 1; 26-50, 2; 51-75, and 3; >75%, 4. Two independent pathologists calculated the H-scores.

Cell lines. In the present study, a normal renal tubular epithelial cell line (HK-2) and RCC cell lines (Caki-1, ACHN, A498, 786-O and 769-P) were purchased from the Chinese Academy of Sciences (Shanghai, China). All cell lines were cultured in 5% CO_2 at 37˚C. The media used were Gibco® McCoy 5A medium, Gibco® RPMI-1640 medium and Dulbecco's modified Eagle's medium (DMEM) (Thermo Fisher Scientific, Inc.). The culture medium contained 10% Gibco® fetal bovine serum and 1% penicillin/streptomycin (Thermo Fisher Scientific, Inc.).

Reverse transcription-quantitative (RT-q) PCR. TRIzol™ (Invitrogen; Thermo Fisher Scientific, Inc.) was used to extract the total RNA of the cell lines, and PrimeScript™ RT Master Mix (Takara Bio, Inc.) was subsequently used to reverse-transcribe the RNA into cDNA according to the manufacturer's instructions. Finally, TB Green® Fast qPCR Mix (Takara Bio, Inc.) was used for RT-qPCR as follows: Pre-denaturation at 95˚C for 30 sec; 40 cycles of denaturation at 95˚C for 5 sec, annealing at 55˚C for 30 sec and extension at 72˚C for 30 sec. mRNA expression levels were quantified using the $2^{-\Delta\Delta Cq}$ method (17), and were standardized against those of β-actin. The primer sequences were as follows: β-actin forward, 5'-GTACGCCAACACAGTGCTG-3' and reverse, 5'-CGT CATACTCCTGCTTGCTG-3'; and ENO2 forward, 5'-AGC CTCTACGGGCATCTATGA-3' and reverse, 5'-TTCTCAGTC CCATCCAACTCC-3'.

Gene ontology (GO) analysis and gene set enrichment analysis (GSEA). According to the median expression level of ENO2, 531 RCC samples from the TCGA cohort were split into groups with high and low ENO2 expression. The 'clusterProfiler' package was used for GO analysis and GSEA (18) in order to further analyze the biological functional differences between the two groups of samples.

Validation of ENO2 function in ccRCC progression in vitro. The RCC cells were transfected with short hairpin (sh)RNAs expressing lentivirus, as per the manufacturer's instructions. The shRNA lentiviral plasmid and its negative control reagents were purchased from TsingKe Biological Technology. shENO2 cells were obtained by antibiotic selection using puromycin (5 μg/ml). The shRNA sequence was as follows: 5'-GCCGGA CATAACTTCCGTAAT-3'. The plasmid used as interference vector was PDS278_pL-U6-shRNA-GFP-ccdB-puro.

Cell counting Kit-8 (CCK-8) cell proliferation assay. The cells were inoculated into 96-well plates (2,000 cells per well) and cultured for 0, 24, 48 and 72 h respectively, prior to evaluation using CCK-8 (10 μl/well, Biosharp Life Sciences). Next, the cells were incubated at 37˚C for 1 h. Finally, the absorbance was measured at 450 nm.

Transwell and Matrigel assays. The cells were suspended in FBS-free medium, and 200 μl cell suspension was inoculated into the wells of the Transwell chamber (Corning, Inc.; $1x10^5$ cells per well). For invasion assay, the Transwell chambers were pre-coated with Matrigel (Corning, Inc.) and incubated at 37˚C for 24 h. Subsequently, 800 μl medium containing 15% FBS was added at the bottom of the chamber.

After 48 h, the cells were treated with 4% paraformaldehyde at room temperature for 20 min. Subsequently, the cells were stained with 0.1% crystal violet at room temperature for 30 min, and finally the cells were washed with PBS. The stained cells were counted and images were captured under an optical microscope.

Western blot analysis of the model. The total protein was extracted from cells by NP-40 Lysis Buffer (Beyotime Institute of Biotechnology, Inc.). The protein concentrations were measured by BCA P rotein Assay Kit (Epizyme, Inc.) according to the manufacturer's instructions. Proteins (30 μg/per lane) were extracted using 10% SDS-PAGE and transferred to a nitrocellulose membrane (Thermo Fisher Scientific, Inc.). The membranes were blocked using Protein Free Rapid Blocking buffer (Epizyme, Inc.) at room temperature for 10 min, and then incubated overnight at 4˚C with the following primary antibodies: ENO2 (1:1,000; cat. no. ab79757; Abcam), N-cadherin (1:1,000; cat. no. A19083), VIM (1:1,000; cat. no. A19607) and β-actin (1:50,000; cat. no. AC026; all from ABclonal Biotech Co., Ltd.). After washing the membrane, a secondary antibody (horseradish peroxidase-conjugated goat anti-rabbit (1:5,000; cat. no. BS13278; Bioworld Technology, Inc.) was added at room temperature for 30 min. Finally, enhanced chemiluminescence reagent (Biosharp Life Sciences) was used to detect the amounts of proteins.

Immune infiltration analysis. Bindea *et al* (19) reported various marker genes of immune cells. The single-sample GSEA (ssGSEA) method was used to analyze the immune infiltration of TCGA samples (20). Finally, the degree of correlation between ENO2 and the aforementioned 24 types of immune cells was analyzed using Pearson's correlation method.

Analysis of the correlation of ENO2 expression with the tumor immune dysfunction and exclusion (TIDE) score. The samples in TCGA dataset were scored using the TIDE algorithm, and the efficacy of ICB was predicted by analyzing the association between ENO2 expression and TIDE score (21).

Statistical methods. The Wilcoxon signed rank test was used for paired samples, and the Wilcoxon rank sum test was used for unpaired samples. Survival curves were constructed, and the survival rate was calculated using the Kaplan-Meier method and the log-rank test. Univariate and multivariate Cox regression analyses were used to determine the independent prognostic factors, and the threshold for the P-value included in multivariate analysis was 0.1. Pearson correlation analysis was used to determine the correlation between ENO2 and the expression levels of other genes. The 'timeROC' package was used to plot the receiver operating characteristic (ROC) curves. The mean ± standard deviation (SD) was used to express numerical data. $P<0.05$ was considered to indicate a statistically significant difference. R language (version 4.0.3, RStudio, lnc.) was used for all statistical analyses.

Results

ENO2 may have a significant role in ccRCC as a hub gene. R language was used to analyze the GSE40435 dataset, and 220 DEGs were screened out (Fig. 1A). The correlation between these DEGs was subsequently analyzed using a string PPI network (Fig. 1B). A total of 30 top genes were screened for possible hub genes based on the results of the Cytoscape software (Fig. 1B and C). The 30 genes were then analyzed according to prognosis in TCGA database, and 16 prognostic genes were screened out (Fig. 1D). The datasets of GSE46699 and GSE53757 were selected to perform the difference analysis, and the top 50 up- and downregulated genes with the highest level of expression were examined. These were found to intersect with GSE40435 to screen ENO2 (Fig. 1E and F), indicating that ENO2 may be a key player in the development of ccRCC as an oncogene.

ENO2 is highly expressed in TCGA and clinical ccRCC cohorts, and its upregulation is associated with clinical prognosis. Subsequently, the expression pattern of ENO2 in the available ccRCC dataset was examined in order to illustrate the potential impact of ENO2. The results of the paired or unpaired sample analysis showed that ENO2 expression was more prominent in ccRCC tissues compared with normal tissues (Fig. 2A and B). Furthermore, low ENO2 expression in patients with ccRCC was associated with improved overall survival (OS) and disease-free survival rates according to the prognostic analyses (Fig. 2C and D). ENO2 expression was identified as a predictor of OS in patients with ccRCC through univariate and multivariate Cox analyses (Table I). Time-dependent ROC analysis revealed that the area under the curve (AUC) was 0.593, 0.626 and 0.679 when the 3-, 5- and 10-year OS rates respectively were taken as the endpoint of the TCGA cohort (Fig. 2E).

The IHC results revealed that ccRCC tissues (n=191) exhibited more positive cells and a higher degree of ENO2 antibody staining compared with the nearby normal tissues (n=177), and a representative IHC image is shown in Fig. 2G. ENO2 expression was found to be a predictor of OS in patients with ccRCC through using univariate and multivariate Cox analyses (Table II). The optimal cut-off number was 6 (H-score) according to AUC, which was calculated using 5-year survival data and was 0.788 (Fig. 2F). In accordance with the cutoff value, the patients were subsequently classified into two groups: The ENO2 high expression group (n=130) and the ENO2 low expression group (n=61). Patients with low expression of ENO2 had superior OS rates according to the Kaplan-Meier analysis (Fig. 2H).

GO and GSEA analysis of ENO2 expression. To further study the underlying molecular mechanism of ENO2 in the progression of ccRCC, 18,521 DEGs were screened from TCGA transcriptome data, and the 2,440 genes whose expression levels were most closely linked with the expression of ENO2 were then extracted. ENO2 was found to be mainly associated with the processes of keratinocyte differentiation, keratinization and epidermal cell differentiation according to GO analysis, and the intracellular locations where ENO2 was mainly active were the nuclear nucleosome, endoplasmic reticulum lumen and cornified envelope (Fig. 3A).

The biological functions associated with ENO2 were subsequently determined by GSEA. These findings

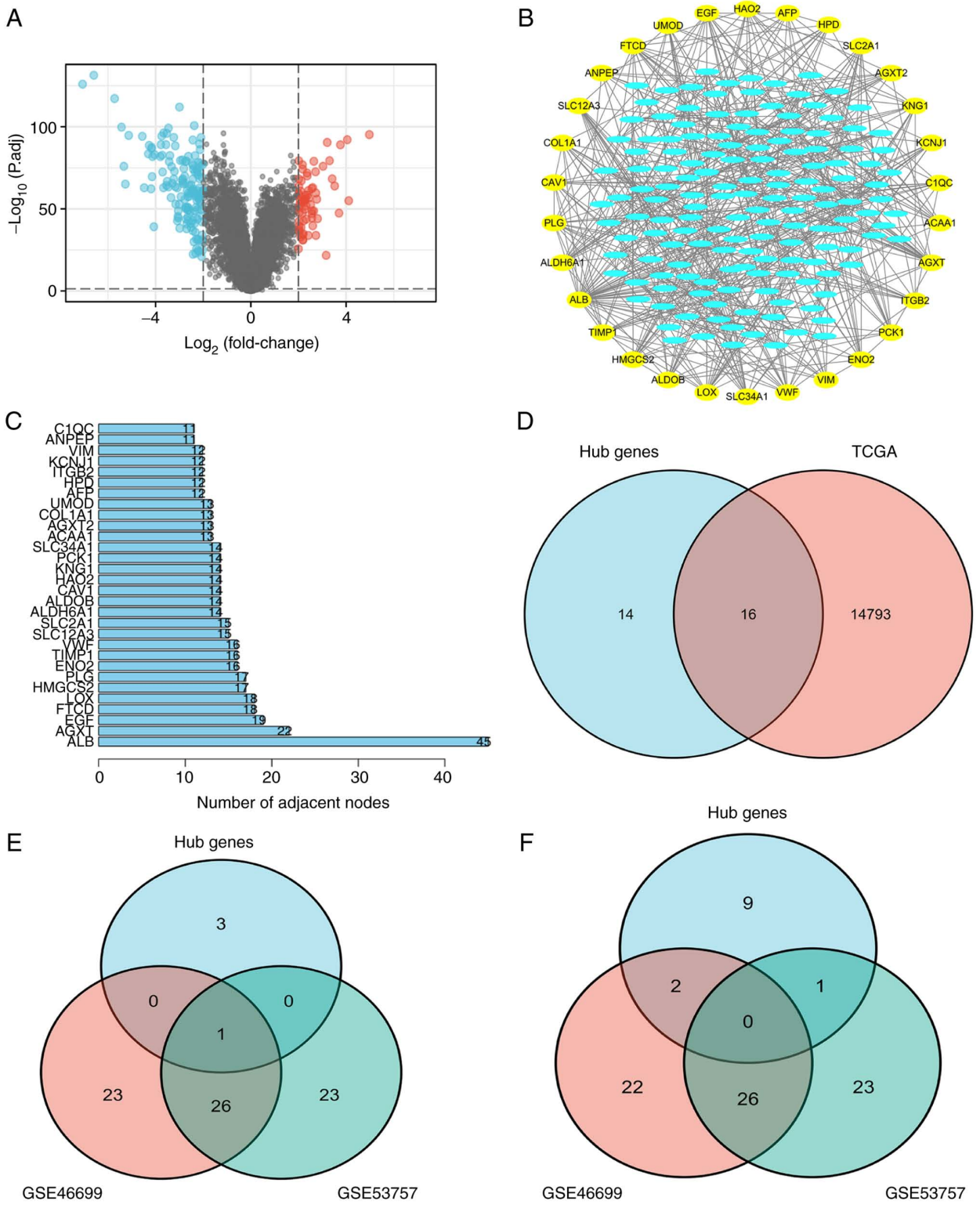

Figure 1. Screening for differential genes via TCGA and the GEO database. (A) Screening of 220 upregulated genes compared with normal tissues in GSE40435 (|log2(FC)|>2, P<0.05). (B and C) By analyzing the association among the 220 DEGs, a PPI network was established. A total of 30 top hub genes were finally selected, which are shown in the outer circle. (D) A total of 16 hub genes associated with prognosis were screened according to TCGA database. (E) Compared with normal tissues, 50 upregulated genes were screened in GSE46699 and GSE53757 (|log2(FC)|>2, P<0.05), and one target gene was screened out. (F) Compared with normal tissues, 50 downregulated genes were screened in GDE46699 and GSE53757 (|log2(FC)|>2, P<0.05), and no hub genes were screened out. GEO, Gene Expression Omnibus; DEG, differentially expressed gene; TCGA, The Cancer Genome Atlas; PPI, protein-protein interaction.

demonstrated that ENO2 was closely correlated with a number of cancer-associated pathways, including EMT, oxidative phosphorylation, fatty acid metabolism, hypoxia and bile acid metabolism (Fig. 3B). Among these, the EMT pathway was found to have the highest enrichment score. Moreover, public data of RCC in TCGA showed that ENO2 expression was highly correlated with multiple currently known EMT marker genes (Fig. 3C).

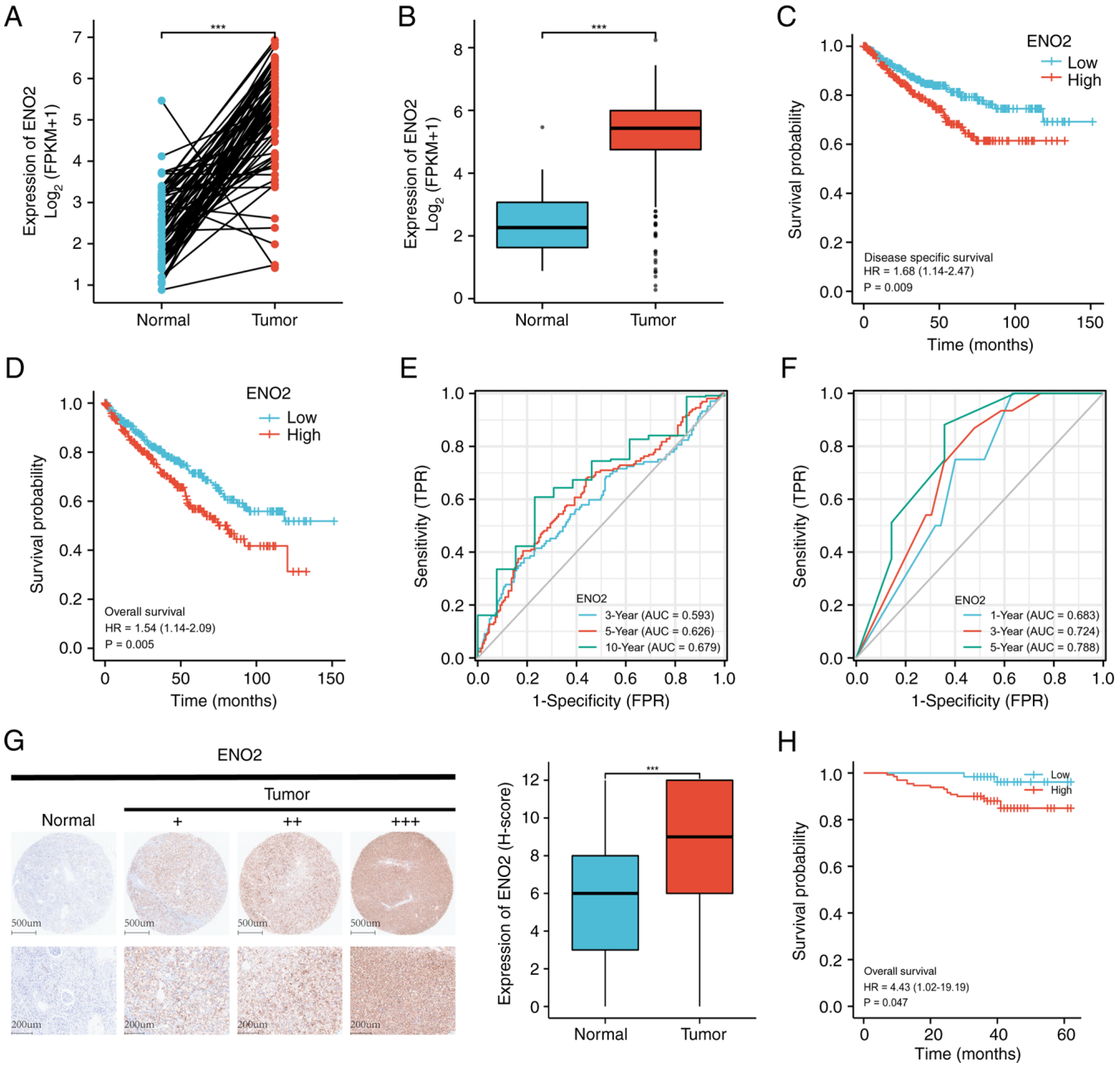

Figure 2. ENO2 high expression is associated with clinical prognosis in ccRCC. (A) ENO2 expression levels in TCGA dataset unpaired samples (P<0.05). (B) ENO2 expression levels in TCGA dataset paired samples (P<0.05). (C) The TCGA dataset's DSS analysis of the ENO2 high- and low-expression groups (P<0.05) is shown. (D) The TCGA dataset's OS analysis of the ENO2 high- and low-expression groups is shown (P<0.05). (E) The ROC curves used in the TCGA cohort to predict the 3-, 5-, and 10-year OS rates of patients with ccRCC based on the ENO2 level. (F) The ROC curves used in the external validation cohort to predict the 1-, 3-, and 5-year OS of patients with ccRCC based on the ENO2 level (H-score). (G) ENO2 expression levels in the external validation cohort (P<0.05) are shown; the IHC images represent ENO2 protein expression in ccRCC and adjacent tissues. (H) The external validation cohort dataset's OS analysis of the ENO2 high- and low-expression groups (P<0.05). ***P<0.001. ENO2, enolase 2; ccRCC, clear cell renal cell carcinoma; TCGA, The Cancer Genome Atlas; ROC, receiver operating characteristic; DSS, disease-free survival; OS, overall survival; IHC, immunohistochemistry analysis.

ENO2 knockdown inhibits EMT and ccRCC progression. To verify the role that ENO2 has in the progression of EMT and ccRCC, the expression level of ENO2 in human normal renal tubular epithelial cells (HK2) and in a panel of ccRCC cell lines (Caki-1, 786-O, 769-P, ACHN and A498) was detected in *in vitro* experiments. These experiments showed that ccRCC cells had considerably greater levels of ENO2 expression compared with HK2 cells (Fig. 4A), a finding that was consistent with our results showing that the expression of ENO2 in ccRCC tissue was greater compared with normal tissue (Fig. 2B). To determine the role of ENO2 in ccRCC, ENO2 knockdown in ACHN and 769-P cells was carried out by performing stable transfections of control shRNA or ENO2 shRNA using lentiviral vectors. E-cadherin, N-cadherin and the EMT-induced transcription factor vimentin (VIM) are three proteins that are often measured to determine the extent of EMT (22). By using western blotting to identify these crucial EMT-associated molecules, the expression levels of N-cadherin and vimentin were found to be markedly decreased when ENO2 was knocked down (Fig. 4B and C). To determine

Table I. Univariate and multivariate analysis of the correlation between ENO2 expression and overall survival in The Cancer Genome Atlas patients with clear cell renal cell carcinoma.

		Univariate analysis		Multivariate analysis	
Characteristics	Total (n)	Hazard ratio (95% CI)	P-value	Hazard ratio (95% CI)	P-value
T stage	539				
T1 and T2	349	Reference			
T3 and T4	190	3.228 (2.382-4.374)	<0.001	1.648 (0.723-3.756)	0.235
N stage	257				
N0	241	Reference			
N1	16	3.453 (1.832-6.508)	<0.001	1.711 (0.857-3.418)	0.128
M stage	506				
M0	428	Reference			
M1	78	4.389 (3.212-5.999)		2.861 (1.679-4.875)	<0.001
Pathologic stage	536				
Stages I and II	331	Reference			
Stages III and IV	205	3.946 (2.872-5.423)	<0.001	1.146 (0.449-2.921)	0.776
Sex	539				
Female	186	Reference			
Male	353	0.930 (0.682-1.268)	0.648		
Age	539				
<=60	269	Reference			
>60	270	1.765 (1.298-2.398)	<0.001	1.725 (1.123-2.652)	0.013
Histologic grade	531				
G1&G2	249	Reference			
G3&G4	282	2.702 (1.918-3.807)	<0.001	1.710 (1.038-2.816)	0.035
ENO2	539	1.317 (1.124-1.544)	<0.001	1.263 (1.033-1.545)	0.023

CI, confidence interval.

the role of ENO2 in cell proliferation, CCK-8 analysis was performed, and the results demonstrated that significantly reduced ENO2 gene activity led to a reduction in the ability of the RCC cell lines to proliferate (Fig. 4D and E). Subsequently, the effect of ENO2 on the migration and invasion of 769-P and ACHN cells was detected using Transwell and Matrigel assay analysis. When compared with the control group, the results demonstrated that ENO2 silencing caused a significant decrease in the migratory and invasive capabilities of the two cell lines (Fig. 4F and G). The aforementioned results implied that ENO2 may influence the EMT process, contributing to the development of ccRCC.

ENO2 is associated with the immune microenvironment of ccRCC. Immune checkpoint therapy is an important method for treating RCC. It is well recognized that EMT is important for the immunosuppression of malignant tumors (23). In the present study, it was hypothesized that ENO2 was associated in some way with the immune microenvironment of RCC. According to the transcriptome data extracted from TCGA ccRCC cohort, the R estimate package was utilized for the immune score computation (24), and this analysis revealed that the immune score was higher in clusters with higher expression levels of ENO2 (Fig. 5A), suggesting that ENO2 may regulate immune cells in the ccRCC microenvironment. Immune cell infiltration in the tumor microenvironment (TME) may affect the efficacy of immunotherapy. Subsequently, the association between 24 different immune cell types and ENO2 expression in the TME was assessed using the ssGSEA method. It was found that ENO2 expression was positively correlated with natural killer (NK) cells, dendritic cells (DCs), CD8 T cells, eosinophils, macrophages, aDCs, Th1 cells, cytotoxic cells and regulatory T cells (Treg) (Fig. 5B). Subsequently, the interactions between ENO2 and numerous key chemokines were examined in order to elucidate the mechanism via which ENO2 may be associated with immune cells. These findings demonstrated a strong correlation between ENO2 expression and the chemokine ligands CCL3, CCL4 and CCL5 (Fig. 5C), which have been demonstrated to be effective regulators of tumor-associated macrophages (TAMs) (25) and tumor-infiltrating neutrophils (TINs) (26). A total of 2 phenotypes of TAM are antitumor M1 macrophages and primitive M2 macrophages. It has been established that a number of carcinogenic pathways can be activated by M2 macrophage polarization to assist in the growth of tumors (27). In addition, in human cancers, neutrophils N1 and N2 perform various roles in different types of human cancer. As a result, it was possible to hypothesize that ENO2 may promote the infiltration of N2

Table II. Univariate and multivariate analysis of the correlation between ENO2 expression and overall survival in Third Affiliated Hospital of the Second Military Medical University patients with clear cell renal cell carcinoma.

		Univariate analysis		Multivariate analysis	
Characteristics	Total (n)	Hazard ratio (95% CI)	P-value	Hazard ratio (95% CI)	P-value
Age	191	1.043 (1.004-1.084)	0.031	1.032 (0.988-1.077)	0.153
Sex	191				
Male	130	Reference			
Female	61	0.741 (0.267-2.058)	0.565		
Fuhrman	191				
Furhman I	25	Reference			
Furhman II	128	1.086 (0.238-4.962)	0.916	0.922 (0.197-4.310)	0.918
Furhman III	24	3.783 (0.762-18.777)	0.104	2.141 (0.388-11.814)	0.383
Furhman IV	14	0.935 (0.085-10.316)	0.956	0.449 (0.039-5.126)	0.519
Stage	191				
Stage 1	154	Reference			
Stage 2	14	4.373 (1.160-16.486)	0.029	3.578 (0.892-14.349)	0.072
Stage 3	22	6.692 (2.426-18.457)	<0.001	5.504 (1.897-15.973)	0.002
Stage 4	1	137.741 (13.295-1427.065)	<0.001	27.013 (2.027-359.924)	0.013
ENO2 (H-score)	191	1.209 (1.021-1.433)	0.028	1.233 (1.031-1.474)	0.022

CI, confidence interval.

neutrophils and M2 macrophages. In the present experiments, it was found that the cell markers for M2 macrophages and N2 neutrophils were favorably linked with ENO2, thereby confirming our conjecture (Fig. 5D and E). Subsequently, the possible correlation between ENO2 and several immunosuppressive markers was examined. It is worth noting that most correlations were found to have a high level of significance, including those with M2 macrophages (CD163 and VISG4) (Fig. 5D) and Treg (CCR8, TGFB1, STAT5b and FOXP3) (Fig. 5F). Depleted T cell markers, such as programmed cell death protein 1 (PDCD1), cytotoxic T-lymphocyte associated protein 4 (CTLA4), lymphocyte activating 3 (LAG3) and hepatitis A virus cellular receptor 2 (HAVCR2), were positively linked with ENO2 expression (Fig. 5G). Collectively, these results suggested that a high expression of ENO2 may regulate the tumor immune response.

Increased expression of ENO2 is associated with higher immune dysfunction scores and poorer efficacy of ICB in patients with ccRCC. To verify the prognostic value of ENO2 for ICB prognosis, TIDE analysis was performed on 531 cases of ccRCC in the ccRCC TCGA cohort. According to this analysis, several immunological checkpoints were found to be significantly associated with ENO2 expression (Fig. 5G). The immune responses of the low expression group of ENO2 were scored more favorably compared with those of the high expression group (Fig. 6A). In addition, increased ENO2 expression was found to be associated with higher immune dysfunction scores, according to Pearson correlation analysis (Fig. 6B) and the TIDE scores (Fig. 6C). Similarly, the high expression of ENO2 was found to predict the poor efficacy of ICB in patients with ccRCC (27.4 cf. 47.7%) (Fig. 6A).

Discussion

In the present study, it has been shown that ENO2 expression was more prominent in ccRCC tissues compared with normal tissues, and ENO2 served a critical function in boosting ccRCC cell migration and proliferation. Moreover, its high expression has been linked to a poor prognosis for patients with ccRCC. GSEA pathway analysis revealed that ENO2 could participate in the regulation of EMT, hypoxia, oxidative phosphorylation, and other pathways in ccRCC cells. The EMT signaling pathway was specifically studied in view of the fact that this pathway showed the highest enrichment score. 'EMT' is the term used to describe the biological process whereby epithelial cells undergo a particular program to change into cells having a mesenchymal character (28). Through the process of EMT, epithelial cells obtain infiltration and metastasis characteristics (29). This constitutes a crucial stage in the spread of malignancies, and EMT is involved in a number of different types of malignant cancers (30). In addition, there are studies reporting that EMT in cancer cells leads to the generation of cancer stem cells, which may contribute to tumor recurrence following treatment (31,32). Downregulation of epithelial-specific markers, a rise in mesenchymal markers, and the development of an invasive phenotype are among the characteristics of EMT. During EMT, the levels of key components, such as E-cadherin, N-cadherin and VIM, are increased significantly (33). Therefore, it was hypothesized that ENO2 may regulate the ccRCC phenotype via regulating the EMT process. The *in vitro* experiments performed in the present study demonstrated that downregulation of the ENO2 gene led to the downregulation of these key factors of EMT. Knockdown of the ENO2 gene was also shown to significantly

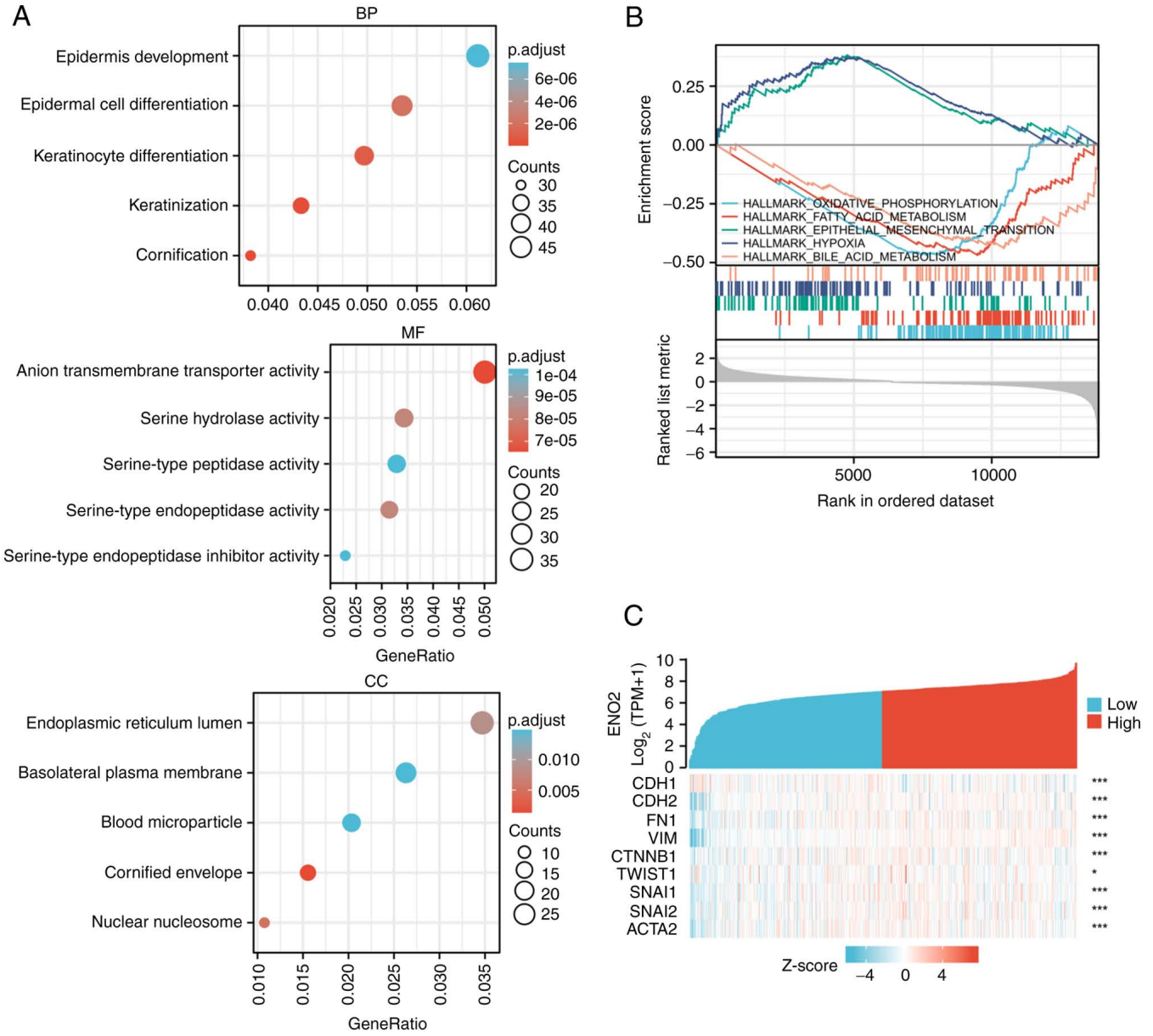

Figure 3. Functional enrichment analysis of ENO2 in ccRCC. (A) GO analysis showing the possible biological functions of ENO2. (B) GSEA analysis showing the signal pathways that ENO2 may participate in. (C) A variety of EMT-related genes are strongly correlated with ENO2. *P<0.05 and ***P<0.001. ENO2, enolase 2; GO, Gene Ontology; GSEA, Gene Set Enrichment Analysis; EMT, epithelial-mesenchymal transition.

reduce the migration, invasion and proliferation of the different ccRCC cell lines.

In addition, EMT is also able to regulate the immune response. In melanoma, EMT has been shown to generate regulatory T cells, resulting in the poor effectiveness of immunotherapy (34). Furthermore, numerous studies have indicated that EMT fulfills a key role in the immunosuppression of malignant tumors (23). As a result, it was possible to hypothesize that ENO2 may be involved in modulating the TME of ccRCC. ccRCC usually has a high level of immune infiltration (35). A variety of immune cells enter the TME to create a vital micro-environment that is involved in numerous aspects of tumorigenesis. Immune cell infiltration in TME was reported to be linked with the prognosis and response to ICB treatment in patients with ccRCC (36,37). In the present study, ENO2 expression was found to be significantly and positively correlated with aDCs, CD8 T cells, cytotoxic cells, eosinophils, DCs, macrophages, Th1 cells, NK cells and Treg. The majority of immune cells in TME congregate in different subsets, and have varying or even opposing functions, depending on the degree and type of illness. Two phenotypes of TAM exist, namely antitumor M1 macrophages and primitive M2 macrophages. A significant aspect of the development of cancer, as demonstrated by a wide number of studies, is the switch from the M1- to the M2-like macrophages (38). N1 and N2 neutrophils fulfill different functions in malignancies. Strong anticancer activity is demonstrated by N1 neutrophils, and through secreting cytokines, these cells may aid in $CD8^{+}$ T cell recruitment and activation (39). The present study revealed a favorable correlation between ENO2 and M2 macrophages and N2 neutrophil markers, suggesting that ENO2 may be associated with the conversion of TAMs

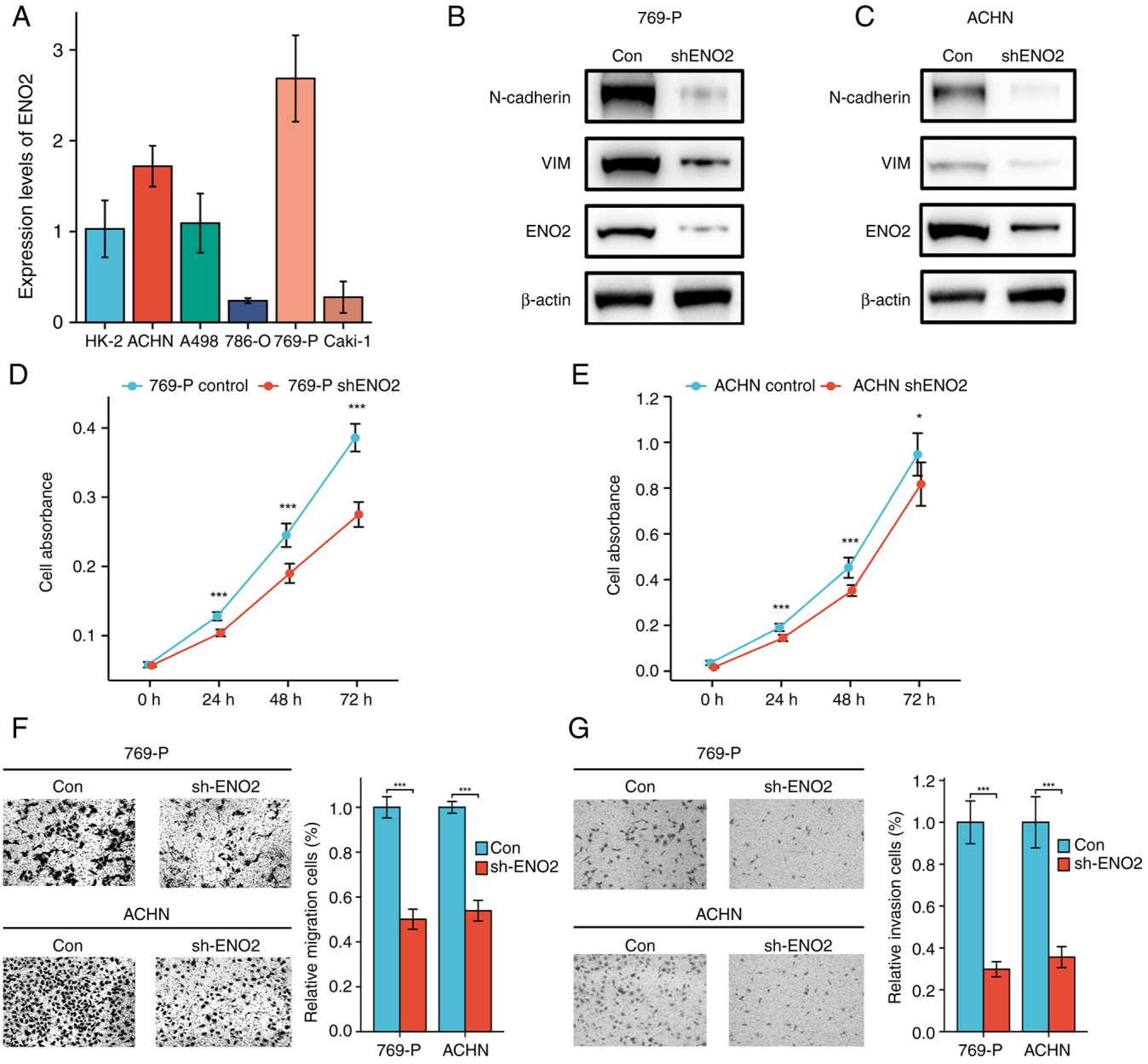

Figure 4. *In vitro* experiments demonstrating that ENO2 knockdown inhibits EMT and ccRCC progression. (A) The mRNA expression levels of ENO2 in HK2 and RCC cells (Caki-1, ACHN, A498, 786-O and 769-P) were detected using reverse transcription-quantitative PCR analysis. (B and C) Western blotting demonstrated that ENO2 expression was effectively knocked down in (B) 769-P and (C) ACHN cells. The altered expression levels of the proteins VIM and N-cadherin suggested that ENO2 knockdown was able to prevent the EMT process of RCC. (D and E) Proliferation of (D) 769-P and (E) ACHN cells transfected with control and shENO2 vectors was determined using Cell Counting Kit-8 assays. (F and G) Two sets of RCC cells (control and shENO2) were tested for their capacity to (A) migrate using Transwell assay analysis and (B) invade using Matrigel assay analysis. Scale bar, 100 μm. *P<0.05 and ***P<0.001. ENO2, enolase 2; EMT, epithelial-mesenchymal transition; ccRCC, clear cell renal cell carcinoma; VIM, vimentin.

and TINs. To examine the association between ENO2 and tumor immunity in more detail, Pearson correlation analysis was used to investigate the correlation between ENO2 and a number of immunological checkpoint molecules, including PDCD1, CTLA4, LAG3 and HAVCR2. Immune checkpoints are a group of molecules that control the level of immune activation, and abnormalities in their expression or function have a significant role in the development of tumors. Due to the activation of immunological checkpoints in tumors, which prevent the antigen presentation process in the TME, immune cells are unable to perform their normal functions (40). A previous study highlighted that ENO2 fulfills an important role in glycolysis in tumors, and silencing or overexpression of ENO2 can significantly decrease or increase lactate levels in the TME, respectively (12). Numerous studies have revealed that excessive lactate in the TME contributes to the establishment of an immunosuppressive environment that favors both tumor cell growth and immune escape (41). Accumulation of lactate in the TME leads to extracellular acidification, and lactic acidosis impairs the function of cytotoxic T lymphocytes through inhibiting T cell receptor-triggered activation of p38 and JNK/c-Jun pathways (42). In addition, increased lactate levels in the TME have been shown to directly inhibit the cytolytic function of NK cells, which are subsequently

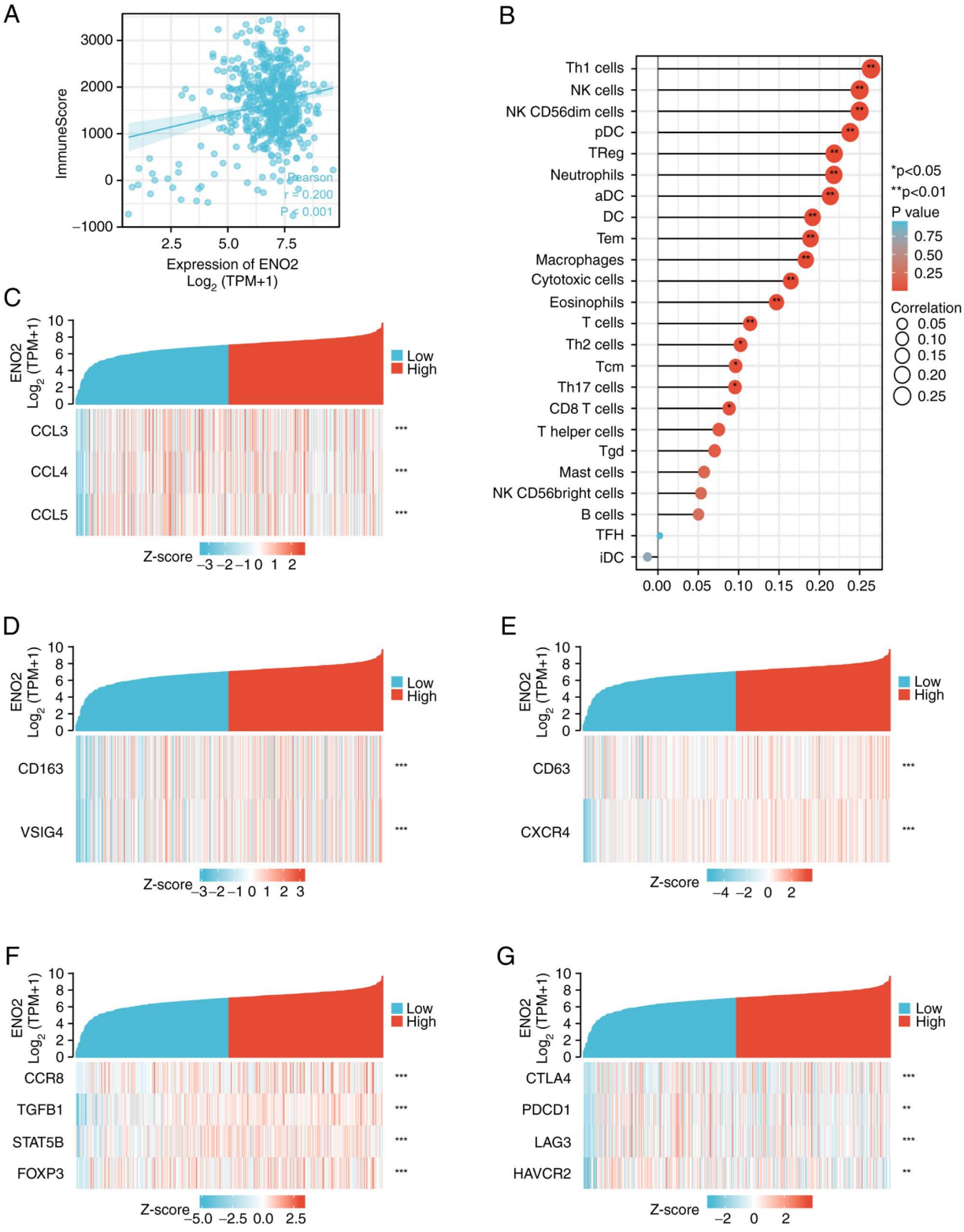

Figure 5. Immune infiltration in patients with ccRCC is correlated with ENO2 expression. (A) ImmuneScore and ENO2 expression level in TCGA patients with ccRCC were analyzed by Pearson correlation analysis. (B) Associations between 24 immune cells and ENO2 expression in ccRCC from TCGA database. (C) Investigation of the association between various chemokines and ENO2. (D) Investigation of the association between cell markers of M2 macrophages and ENO2. (E) Investigation of the association between cell markers of N2 macrophages and ENO2. (F) Investigation of the association between cell markers of Tregs and ENO2. (G) Investigation of the association between immune modulators and ENO2. Pearson's correlation analysis was used to calculate the r and P-values. *P<0.05, **P<0.01 and ***P<0.001. ccRCC, clear cell renal cell carcinoma; ENO2, enolase 2; TCGA, The Cancer Genome Atlas; Treg, regulatory T cell.

able to induce the differentiation of monocytes into DCs with an immunosuppressive phenotype (43-45). Moreover, lactic acidosis has been shown to inhibit the function of M1 macrophages through decreasing the expression of CCL2 and IL-6 (46). Therefore, it was possible to hypothesize that ENO2 affects tumor immune cell infiltration by regulating the level

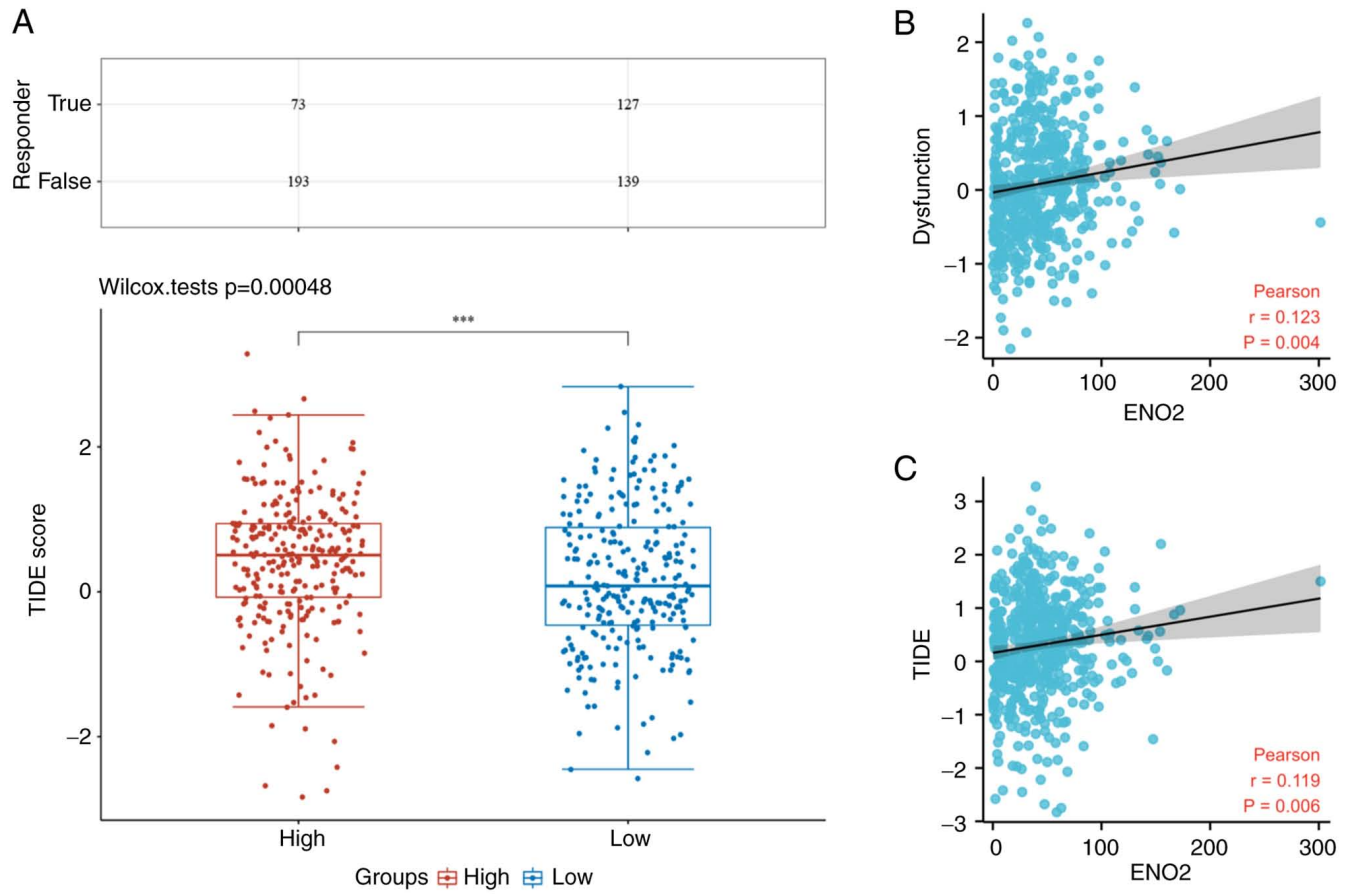

Figure 6. Elevated ENO2 levels are associated with a greater immune dysfunction score and less effective immune checkpoint treatments. (A) Statistical table of immune response of TCGA samples. In the ENO2 high expression and low expression groups, the effective rates of immune checkpoint block were 27.4 cf. 47.7% (P<0.05). The prediction of TIDE scores in low and high expression groups of ENO2. (B) Investigation of the association between immune dysfunction score and ENO2. (C) Investigation of the association between TIDE score and ENO2. Pearson's correlation analysis was used to calculate r and P-values. ***P<0.001. ENO2, enolase 2; TCGA, The Cancer Genome Atlas; TIDE, Tumor Immune Dysfunction and Exclusion.

of lactic acid in TME, which therefore fulfills a key role in the immunosuppression of ccRCC.

At the end of the 19th century, the idea of tumor immunotherapy was initially proposed. It alludes to a form of therapy that eliminates cancer cells by utilizing the autoimmune system. However, it is difficult to assess the efficacy of these blockades (47). The prognosis of tumor patients is significantly impacted by the immunological infiltration of various types of immune cells in the tumor (48). Recent studies have identified two unique tumor immune evasion pathways (49,50). Infiltrating T cells are eliminated by immune-suppressive factors in certain tumors, although in others, significant levels of cytotoxic T cell infiltration are present (51). Peng *et al* (21) created a new computational framework to integrate the two tumor immune escape mechanisms through the TIDE score. These two distinct tumor immune escape pathways are assessed by TIDE using a collection of gene expression indicators, and a higher TIDE score denotes a less effective ICB therapy. A favorable correlation between the immune dysfunction score and the TIDE score, and the expression of ENO2 was identified in the present study. In the present study, the low expression group of ENO2 was found to have a 20.3% higher response rate to immune checkpoint therapy compared with the high expression group, which suggested that patients who express less ENO2 may benefit more from ICB treatment.

In conclusion, the present study has emphasized the clinical significance of ENO2 in ccRCC, and its possible mechanism has been discussed. It was found that ENO2 could regulate the EMT process and regulate the proliferation, metastasis and invasion of ccRCC. In addition, ENO2 was shown to be associated with the immune score of ccRCC. Finally, the present study has disclosed the correlation between ENO2 and tumor immunosuppression, and has also suggested that ENO2 may be used as a potential predictor of the efficacy of ICB.

Acknowledgements

Clinical specimens of RCC were provided by Third Affiliated Hospital of the Second Military Medical University.

Funding

The present study was sponsored by the National Natural Science Foundation of China (grant nos. 81974391, 82072806 and 82173265), the Program of Shanghai Academic/Technology Research Leader (grant no. 19XD1405100), the Clinical Research Plan of SHDC (grant no. SHDC2020CR4025), the Shanghai 'Rising Stars of Medical Talent' Youth Development Program: Youth Medical Talents-Specialist Program, the Shanghai

Municipal Commission of Health and Family Planning (grant no. 20204Y0042), the Technology Project of Jiading Health System (grant no. 2019-QN-03), the Natural Science Foundation of Shanghai (grant no. 20ZR1470500) and the Hospital Funded Clinical Research, Xin Hua Hospital Affiliated to Shanghai Jiao Tong University School of Medicine (grant no. 21XHDB06).

Availability of data and materials

All data generated or analyzed during this study are included in this published article.

Authors' contributions

XGC, XWP and XS were responsible for the conception and design of the present study. XWP, WJC, KQD, JXC and WYL were responsible for the development of the methodology. WJC and WY performed experiments. WY, MG, YH, DX, WJC, and YQW were responsible for analysis and interpretation of the data. XGC, XWP and XS supervised the study. WJC and XWP confirm the authenticity of all the raw data. All authors have read and approved the final manuscript.

Ethics approval and consent to participate

The present study was approved (approval no. EHBHKY2021-01-005) by the ethics committee of Second Military Medical University (Shanghai, China). Written informed consent was obtained from all patients.

Patient consent for publication

Not applicable.

Competing interests

The authors declare that they have no competing interests.

References

1. Grivennikov S, Greten F and Karin M: Immunity, inflammation, and cancer. Cell 140: 883-899, 2010.
2. Baldewijns MM, van Vlodrop IJ, Schouten LJ, Soetekouw PM, de Bruïne AP and van Engeland M: Genetics and epigenetics of renal cell cancer. Biochim Biophys Acta 1785: 133-155, 2008.
3. Fisher R, Gore M and Larkin J: Current and future systemic treatments for renal cell carcinoma. Semin Cancer Biol 23: 38-45, 2013.
4. Fernández-Pello S, Hofmann F, Tahbaz R, Marconi L, Lam TB, Albiges L, Bensalah K, Canfield SE, Dabestani S, Giles RH, *et al*: A systematic review and meta-analysis comparing the effectiveness and adverse effects of different systemic treatments for non-clear cell renal cell carcinoma. Eur Urol 71: 426-436, 2017.
5. Barretina J, Caponigro G, Stransky N, Venkatesan K, Margolin AA, Kim S, Wilson CJ, Lehár J, Kryukov GV, Sonkin D, *et al*: The cancer cell line encyclopedia enables predictive modelling of anticancer drug sensitivity. Nature 483: 603-607, 2012.
6. Vizin T and Kos J: Gamma-enolase: A well-known tumour marker, with a less-known role in cancer. Radiol Oncol 49: 217-226, 2015.
7. Levin VA, Panchabhai SC, Shen L, Kornblau SM, Qiu Y and Baggerly KA: Different changes in protein and phosphoprotein levels result from serum starvation of high-grade glioma and adenocarcinoma cell lines. J Proteome Res 9: 179-191, 2010.
8. Yan T, Skaftnesmo KO, Leiss L, Sleire L, Wang J, Li X and Enger PØ: Neuronal markers are expressed in human gliomas and NSE knockdown sensitizes glioblastoma cells to radiotherapy and temozolomide. BMC Cancer 11: 524, 2011.
9. Hafner A, Obermajer N and Kos J: γ-1-Syntrophin mediates trafficking of γ-enolase towards the plasma membrane and enhances its neurotrophic activity. Neurosignals 18: 246-258, 2010.
10. Hafner A, Obermajer N and Kos J: γ-Enolase C-terminal peptide promotes cell survival and neurite outgrowth by activation of the PI3K/Akt and MAPK/ERK signalling pathways. Biochem J 443: 439-450, 2012.
11. Sturgeon C: Practice guidelines for tumor marker use in the clinic. Clin Chem 48: 1151-1159, 2002.
12. Sun C, Liu M, Zhang W, Wang S, Qian G, Wang M and Zhang G: Overexpression of enolase 2 is associated with worsened prognosis and increased glycikolysis in papillary renal cell carcinoma. J Cell Physiol 236: 3821-3831, 2021.
13. Szklarczyk D, Gable A, Lyon D, Junge A, Wyder S, Huerta-Cepas J, Simonovic M, Doncheva NT, Morris JH, Bork P, *et al*: STRING v11: Protein-protein association networks with increased coverage, supporting functional discovery in genome-wide experimental datasets. Nucleic Acids Res 47 (D1): D607-D613, 2019.
14. Chin CH, Chen SH, Wu HH, Ho CW, Ko MT and Lin CY: cytoHubba: Identifying hub objects and sub-networks from complex interactome. BMC Syst Biol 8 (Suppl 4): S11, 2014.
15. Maere S, Heymans K and Kuiper M: BiNGO: A cytoscape plugin to assess overrepresentation of gene ontology categories in biological networks. Bioinformatics 21: 3448-3449, 2005.
16. Wang C, Peng G, Huang H, Liu F, Kong DP, Dong KQ, Dai LH, Zhou Z, Wang KJ, Yang J, *et al*: Blocking the feedback loop between neuroendocrine differentiation and macrophages improves the therapeutic effects of enzalutamide (MDV3100) on prostate cancer. Clin Cancer Res 24: 708-723, 2018.
17. Livak KJ and Schmittgen TD: Analysis of relative gene expres-sion data using real-time quantitative PCR and the 2(-Delta Delta C(T)) method. Methods 25: 402-408, 2001.
18. Subramanian A, Tamayo P, Mootha VK, Mukherjee S, Ebert BL, Gillette MA, Paulovich A, Pomeroy SL, Golub TR, Lander ES and Mesirov JP: Gene set enrichment analysis: A knowledge-based approach for interpreting genome-wide expression profiles. Proc Natl Acad Sci USA 102: 15545-15550, 2005.
19. Bindea G, Mlecnik B, Tosolini M, Kirilovsky A, Waldner M, Obenauf AC, Angell H, Fredriksen T, Lafontaine L, Berger A, *et al*: Spatiotemporal dynamics of intratumoral immune cells reveal the immune landscape in human cancer. Immunity 39: 782-795, 2013.
20. Hänzelmann S, Castelo R and Guinney J: GSVA: Gene set variation analysis for microarray and RNA-seq data. BMC Bioinformatics 14: 7, 2013.
21. Jiang P, Gu S, Pan D, Fu J, Sahu A, Hu X, Li Z, Traugh N, Bu X, Li B, *et al*: Signatures of T cell dysfunction and exclusion predict cancer immunotherapy response. Nat Med 24: 1550-1558, 2018.
22. Singh M, Yelle N, Venugopal C and Singh SK: EMT: Mechanisms and therapeutic implications. Pharmacol Ther 182: 80-94, 2018.
23. Jiang Y and Zhan H: Communication between EMT and PD-L1 signaling: New insights into tumor immune evasion. Cancer Lett 468: 72-81, 2020.
24. Yoshihara K, Shahmoradgoli M, Martínez E, Vegesna R, Kim H, Torres-Garcia W, Treviño V, Shen H, Laird PW, Levine DA, *et al*: Inferring tumour purity and stromal and immune cell admixture from expression data. Nat Commun 4: 2612, 2013.
25. Eissmann M, Dijkstra C, Jarnicki A, Phesse T, Brunnberg J, Poh AR, Etemadi N, Tsantikos E, Thiem S, Huntington ND, *et al*: IL-33-mediated mast cell activation promotes gastric cancer through macrophage mobilization. Nat Commun 10: 2735, 2019.
26. Mukaida N, Sasaki SI and Baba T: CCL4 signaling in the tumor microenvironment. Adv Exp Med Biol 1231: 23-32, 2020.
27. Lan J, Sun L, Xu F, Liu L, Hu F, Song D, Hou Z, Wu W, Luo X, Wang J, *et al*: M2 macrophage-derived exosomes promote cell migration and invasion in colon cancer. Cancer Res 79: 146-158, 2019.
28. Yang J, Antin P, Berx G, Blanpain C, Brabletz T, Bronner M, Campbell K, Cano A, Casanova J, Christofori G, *et al*: Author correction: Guidelines and definitions for research on epithelial-mesenchymal transition. Nat Rev Mol Cell Biol 22: 834, 2021.
29. Mittal V: Epithelial mesenchymal transition in tumor metastasis. Annu Rev Pathol 13: 395-412, 2018.

30. Bai J, Zhang X, Shi D, Xiang Z, Wang S, Yang C, Liu Q, Huang S, Fang Y, Zhang W, *et al*: Exosomal miR-128-3p promotes epithelial-to-mesenchymal transition in colorectal cancer cells by targeting FOXO4 via TGF-β/SMAD and JAK/STAT3 signaling. Front Cell Dev Biol 9: 568738, 2021.
31. Morel A, Lièvre M, Thomas C, Hinkal G, Ansieau S and Puisieux A: Generation of breast cancer stem cells through epithelial-mesenchymal transition. PLoS One 3: e2888, 2008.
32. Shibue T and Weinberg RA: EMT, CSCs, and drug resistance: The mechanistic link and clinical implications. Nat Rev Clin Oncol 14: 611-629, 2017.
33. Thiery JP, Acloque H, Huang RY and Nieto MA: Epithelial-mesenchymal transitions in development and disease. Cell 139: 871-890, 2009.
34. Kudo-Saito C, Shirako H, Takeuchi T and Kawakami Y: Cancer metastasis is accelerated through immunosuppression during Snail-induced EMT of cancer cells. Cancer Cell 15: 195-206, 2009.
35. Díaz-Montero CM, Rini BI and Finke JH: The immunology of renal cell carcinoma. Nat Rev Nephrol 16: 721-735, 2020.
36. Tran Janco JM, Lamichhane P, Karyampudi L and Knutson KL: Tumor-infiltrating dendritic cells in cancer pathogenesis. J Immunol 194: 2985-2991, 2015.
37. Stanton SR and Disis ML: Clinical significance of tumor-infiltrating lymphocytes in breast cancer. J Immunother Cancer 4: 59, 2016.
38. Pandey G: Tumor-associated macrophages in solid tumor: Friend or foe. Ann Transl Med 8: 1027, 2020.
39. Fridlender ZG and Albelda SM: Tumor-associated neutrophils: Friend or foe? Carcinogenesis 33: 949-955, 2012.
40. Zeng D, Li M, Zhou R, Zhang J, Sun H, Shi M, Bin J, Liao Y, Rao J and Liao W: Tumor microenvironment characterization in gastric cancer identifies prognostic and immunotherapeutically relevant gene signatures. Cancer Immunol Res 7: 737-750, 2019.
41. Wang ZH, Peng WB, Zhang P, Yang XP and Zhou Q: Lactate in the tumour microenvironment: From immune modulation to therapy. EBioMedicine 73: 103627, 2021.
42. Xia H, Wang W, Crespo J, Kryczek I, Li W, Wei S, Bian Z, Maj T, He M, Liu RJ, *et al*: Suppression of FIP200 and autophagy by tumor-derived lactate promotes naïve T cell apoptosis and affects tumor immunity. Sci Immunol 2: eaan4631, 2017.
43. Husain Z, Seth P and Sukhatme VP: Tumor-derived lactate and myeloid-derived suppressor cells: Linking metabolism to cancer immunology. Oncoimmunology 2: e26383, 2013.
44. Erra Díaz F, Ochoa V, Merlotti A, Dantas E, Mazzitelli I, Gonzalez Polo V, Sabatté J, Amigorena S, Segura E and Geffner J: Extracellular acidosis and mTOR inhibition drive the differentiation of human monocyte-derived dendritic cells. Cell Rep 31: 107613, 2020.
45. Nasi A, Fekete T, Krishnamurthy A, Snowden S, Rajnavölgyi E, Catrina AI, Wheelock CE, Vivar N and Rethi B: Dendritic cell reprogramming by endogenously produced lactic acid. J Immunol 191: 3090-3099, 2013.
46. Certo M, Tsai CH, Pucino V, Ho PC and Mauro C: Lactate modulation of immune responses in inflammatory versus tumour microenvironments. Nat Rev Immunol 21: 151-161, 2021.
47. Marin-Acevedo JA, Dholaria B, Soyano AE, Knutson KL, Chumsri S and Lou Y: Next generation of immune checkpoint therapy in cancer: New developments and challenges. J Hematol 11: 39, 2018.
48. Gentles AJ, Newman AM, Liu CL, Bratman SV, Feng W, Kim D, Nair VS, Xu Y, Khuong A, Hoang CD, *et al*: The prognostic landscape of genes and infiltrating immune cells across human cancers. Nat Med 21: 938-945, 2015.
49. Gajewski TF, Schreiber H and Fu YX: Innate and adaptive immune cells in the tumor microenvironment. Nat Immunol 14: 1014-1022, 2013.
50. Joyce JA and Fearon DT: T cell exclusion, immune privilege, and the tumor microenvironment. Science 348: 74-80, 2015.
51. Spranger S and Gajewski TF: Tumor-intrinsic oncogene pathways mediating immune avoidance. Oncoimmunology 5: e1086862, 2016.